



## Case Study

# Experimental and statistical investigation on the performance of asphalt overlays reinforced with geocomposite in controlling the reflective cracks under different loadings and temperatures

Saeid Asadi<sup>1</sup> · Gholamali Shafabakhsh<sup>1</sup>

Received: 10 February 2023 / Accepted: 14 June 2023

Published online: 03 July 2023

© The Author(s) 2023 **OPEN**

## Abstract

One of the easiest method to repair the old pavement is to apply an overlay on them. However, the deteriorated pavement affects the overlay performance by propagating the existing cracks upwards to the overlay due to the stress and strain concentration from the loading and temperature variations. Today, using the asphalt overlays reinforced with geosynthetic interlayers is one of the most effective methods to prevent the reflective cracking. This paper investigates the effects of the temperature, bending fatigue loading frequency and geocomposite tensile strength on the asphalt overlays performance experimentally. The crack initiation and its propagation rate were analyzed by the help of image processing technique and statistically. The obtained results revealed that the temperature has the greatest effect on the reflective cracking rate, so that by increasing the temperature from 20 to 40 °C in addition to increasing the crack growth rate and changing the vertical deformation under the load, the direction of crack formation changes, and besides the reflective cracks, the top-down cracks also appear. Furthermore at the higher loading frequency more than 10 Hz, even in samples reinforced with geocomposite, increasing the temperature from 0 to 20 and 40 °C will increase the crack growth rate between 5 and 30 times. The obtained coefficients of determination ( $R^2$ ) and Adjusted  $R^2$  are equal to 0.9936 and 0.9907, respectively, indicating the satisfactory prediction of the model compared to the real observations.

**Keywords** Reflective crack · Geocomposite · Reinforced overlay · Statistical analysis · Image analysis · Cracking rate

## 1 Introduction

Pavement overlay is one of the most basic methods of the road maintenance. However, applying of a new asphalt concrete overlay on the old pavement with cracks will lead to road cracking with a pattern similar to the existing ones [1–3]. These types of cracks are called reflective cracks. Considering the constant environmental conditions and the loading pattern, it can be stated that generally after implementing a new asphalt concrete overlay on the previous pavement, the new cracks will appear on

the new overlay after a short time. Therefore, these structural defects will damage the new overlay [4–7]. According to the Texas Department of Transportation (TxDOT), the reflective crack is one of the most serious damages affecting the asphalt overlay and concrete pavements [8].

Regarding the nature of such defects, various opinions have been stated about their origin and conditions. These defects are also likely to occur in asphalt overlays laid on the cement concrete slabs. These cracks are mainly created due to displacement caused by heat or humidity in the concrete slab under the asphalt overlay. Although the

✉ Gholamali Shafabakhsh, ghshafabakhsh@semnan.ac.ir; Saeid Asadi, saeid.asadi@semnan.ac.ir | <sup>1</sup>Faculty of Civil Engineering, Semnan University, Semnan 3513119111, Iran.



origin of cracking is not always the traffic loading, it may cause failures and cracks near the joints [9–11]. According to “Asphalt concrete modeling book” by Kim, when a pavement overlay is applied on the existing concrete pavement (semi-rigid structure), some cracks appear due to concrete pavement shrinkage, thermal displacements, or lateral displacements in concrete pavement. Generally, the asphalt overlay layers cannot tolerate high displacements without the damage and cracking. Therefore, the cracks from the joints existing in the concrete pavement or in the old asphalt layer spread out gradually with the destruction of the new asphalt overlay and reach to the overlay surface along its thickness (reflective cracking) [12]. Today, various methods are available to prevent or delay the occurrence of reflective cracks. Overall, these methods can be classified into the following three categories: 1) Reinforcing the overlay, 2) Reducing the stress through installing stress absorbing membrane interlayer (SAMI), and 3) Repairing and restoring the resistance of the underlying pavement to the time before the overlay was applied.

Prevention of the stress concentration in the newly applied pavement (top layer) can significantly reduce the occurrence of the reflective cracks. Therefore, the researchers have considered several methods to deal with the reflective cracking phenomenon; for example, using the asphalt with wide and non-uniform aggregate gradation, warm mix asphalt (WMA) with the low viscosity, embedding a modified SAMI, and fabrics interlayer that can reduce strains [13].

In this regard, the results of an extensive study on the different stress-absorbing interlayers by Zhang et al. showed that the rubber asphalt can be considered as a suitable mixture for the stress-absorbing layer due to its high elasticity and resistance to fatigue. Also, the results showed that the interlayer shear resistance curve reaches to its maximum value when the asphalt application rate is 2.2 kg/m. According to the cracking data, the fatigue and rupture life of asphalt overlays with rubber stress absorbing interlayer on the old concrete pavement increased by 30 percent [14].

The pavement reinforcement and stress reduction on the pavement layers are the key functions of the geosynthetic materials in road construction projects. The most important advantages of using the geosynthetic materials in asphalt overlay are the stress and displacement reduction on the pavement structure. So, using the geosynthetic materials on the pavement can delay or control some types of cracks including reflective cracks as a stress-reducing layer [15]. Researchers have evaluated the feasibility of the geosynthetic materials' effect in reducing and delaying the reflective cracks [16]. In addition, some geocomposites have been analyzed as an interlayer in

finite element modeling (FEM) for the different designs of asphalt overlay, and their ability to reduce the reflective cracks has been evaluated. Based on the observations, as long as using the geocomposite as an intermediate layer, the asphalt pavement remains healthy without sustaining any damage. In other words, the crack does not pass through the pavement, and the energy generated at the crack tip is dissipated. This membrane serves as a protective shield against the crack tip [17]. In another research on the efficiency of geosynthetics using the 4-point bending test at 20°C, it was found that the composite samples with modified and reinforced asphalt overlays present the higher fatigue life performance than other samples even in heavier traffic loads [18]. The results of an experimental study by a group of transportation researchers showed that in all geocomposite-reinforced specimens, the permanent deformation resistance increased compared to the control samples. Besides, geocomposites reduce the energy required for the crack propagation in thin layer overlays by 3 times [19].

Another role of geosynthetics used in road maintenance is the pavement reinforcing. The geosynthetics, especially geogrids, increase the resistance of the pavement by changing the load distribution pattern and aggregate's behavior against the load after being implemented in asphalt overlays. Using geogrids with the high tensile strength in pavements can be assumed as a network of rebars in reinforced concrete that prevent the crack propagation in the asphalt overlay [20, 21]. In an advanced laboratory investigation, Çelik et al. (2021) found that using asphalt overlay reduces the vertical displacement in concrete surfaces by 2 to 75%. Furthermore, applying geogrid reinforcement on the developed cracks reduces the strain in the bottom of the asphalt layer from 29.5% to 92.5%. Moreover, using geogrid on the joints instead of increasing asphalt layer thickness from 50 to 80 mm, decreases the strain, displacement, and the overall cost by 57.9 percent [22].

Furthermore, the deformation of geogrids in the pavement causes energy dissipation in the crack tip area, which means preventing the progressive destruction in the pavement properly [20, 21]. Regarding the excellent performance of geogrids in controlling the reflective pavement cracks, many studies have been recently conducted on the effect of different parameters on the pavement performance [23–26]. The geogrid overlay reinforcement can significantly reduce the crack propagation from the bottom to the top layer. It is noteworthy that the pavement reinforcement would be effective only when the geosynthetic modulus is more than the asphalt layer modulus. Also, it should sufficiently bond to the surrounding asphalt material to strengthen the asphalt overlay [4, 15]. In this regard, Kikwata and Muramatsu (1989) investigated the degree

of connection and continuity of geosynthetics with the surrounding asphalt pavement. The results revealed that the geosynthetics hardness indicates the greatest effect in achieving proper overlay performance [27]. The pavement reinforcement can be accomplished using the geosynthetic layer either in the pavement's lower layers (i.e., aggregate pavement layers such as the base and sub-base) or in its asphalt layer. In any case, to control the reflective cracks, it is necessary to implement the geosynthetic layer in the overlay layer [28]. The type of old cracked pavement (either asphalt or concrete), the location of the geogrid layer in the pavement, and the weather temperature of the pavement site are the most critical factors affecting the cracking rate [4].

Another important parameter of geosynthetics in controlling reflective cracks is the type of loading applied to the pavement complex. In this respect, some experiments have been conducted with the static and dynamic loadings by constant strain on the asphalt overlay reinforced with geogrid. Based on the obtained results, the hardness and bearing capacity of the asphalt overlay before cracking increase with geogrid installation. It should be mentioned that this increase for the sample under dynamic loading is much higher than the similar sample under the static loading [29]. Therefore, it can be concluded that the effect of using geosynthetics in cracking rate and increasing the hardness of the pavement layer under static loading (e.g., parking lots) is far less than areas under dynamic loading (e.g., highways and high traffic areas) [29]. Gonzalez-Torre et al. (2015) investigated the role of type-in geosynthetic in cracking behavior and reported that the geosynthetic elastic modulus is not the only determining factor in controlling the reflective cracks [30]. Finally, it can be said that the anti-reflective cracking systems can be developed by geosynthetics with a high elastic modulus (e.g., geogrid) between asphalt overlays. Considering the gap in past researches, in this paper, it was tried to investigate the crack growth in the asphalt shaped slab samples with different geocomposite and control interlayers under various cyclic dynamic loadings in the opening or bending mode. Also, the speed index and crack growth rate in asphalt pavements with geocomposite or control reinforcements were modeled using the statistical regression method. It should be mentioned that these models are based on the mechanistic-experimental relationships in evaluating the fatigue life, crack growth rate, and etc. in asphalt overlays with geosynthetic materials to delay the reflective cracks. Also, in this paper, for a comprehensive and innovative investigation, the variables of temperature and loading intensity (frequency) in different time intervals were used to better simulate the reflective crack tests on the performance of such geosynthetic reinforcements. The obtained results are applicable in predicting

the performance of pavements in different temperature ranges and frequency ranges.

## 1.1 Objective

In this research, the cyclic bending fatigue tests are performed to study the cracking rate in the asphalt overlay by considering the effect of temperature, loading frequency, and different geocomposites. Also, models for predicting the cracking rate based on the mentioned parameters are established using the statistical analyses. Furthermore, to simulate an old crack, a 1.2-mm wide crack is created in the bottom layer in all samples.

## 2 Materials and methods

In the ensuing pages, the conventional properties of used aggregates, asphalt binder along with sample preparation methods are provided.

### 2.1 Materials

The aggregate was obtained from the Qazvin Axis Asphalt Pavement Factory. Located in Abyek city, Alborz, Iran. The aggregate gradation is shown in Fig. 1. Also, a PG 64–22 asphalt binder provided by the Tehran Refinery Inc., was then used to prepare hot asphalt mixture. The conventional properties of the asphalt binder is shown in Table 1. The mix design for all asphalt overlay samples was based on the Marshall Construction Standard (ASTM D 1559) and according to the obtained data from Marshall's tests, in this research the optimum bitumen percentage was determined 4.55% by the weight of mixture.

Also, in this research two types of geocomposite as shown in Fig. 2 were used with characteristics provided in Table 2.

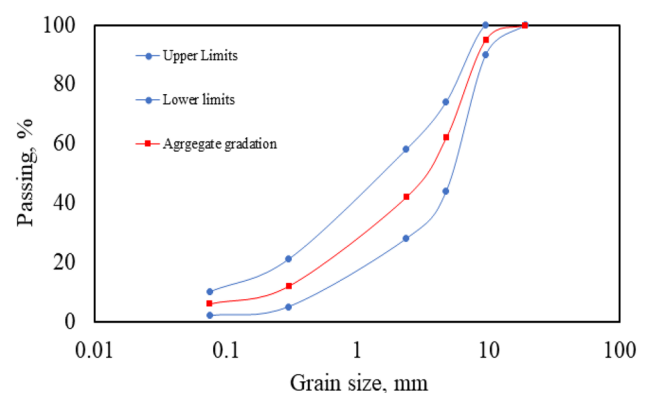
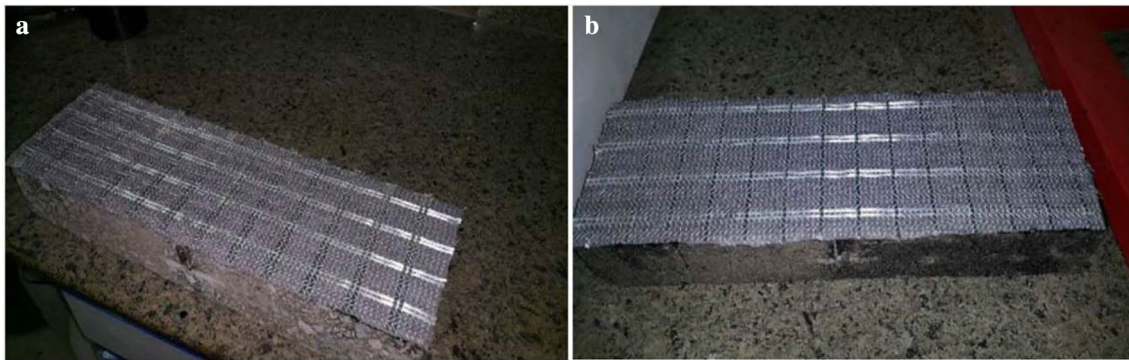


Fig. 1 Aggregate gradation used in asphalt samples



**Fig. 2** Two geocomposite types used in this study, **a** GI: geocomposite 100–100, **b** GII: geocomposite 50–50

**Table 1** Specifications of bitumen used for the preparation of two-layer asphalt slabs

Properties	Standard		Results
	ASTM	AASHTO	
Specific gravity, N/m <sup>3</sup>	D70	T228	1.020
Penetration, mm	D5	T49	60
Minimum softening point (ring-ball), °C	D36	T53	49.4
Stretch level at 25°C, cm	D113	T51	> 100
Flashpoint, °C	D92	T48	320
Kinematic viscosity at 120°C, cSt	D2170	T201	676
Kinematic viscosity at 135°C; cSt	D2170	T201	311
Kinematic viscosity at 160°C; cSt	D2170	T201	153

**Table 2** Geocomposite properties as an interlayer for asphalt pavements

Sample ID	Bitumen to adhere the interlayer to the asphalt overlays (kg/m <sup>2</sup> )	Tensile strength in direction 1 (kN/m)	Tensile strength in direction 2 (kN/m)
GI: type-I	0.9	100	100
GII: type-II	0.9	50	50

## 2.2 Samples construction

To prepare the samples, two asphalt slabs were attached to each other with or without geocomposite using Pres-Box compression-shear compactor as illustrated in Fig. 3. The sample preparation was based on the vertical and shear stresses applied to the sample, air percentage, density (specific gravity), and loading time [4, 24, 31–33]. The modified emulsion bitumen with fragile SBS polymer was employed on the top of 7 cm slab as the bottom layer to create a surface pavement (single coat) and the geocomposite layer was placed on that. Then, the typical 5 cm

overlay layer was applied to it. As earlier mentioned, the crack with 1.2 mm width has been created as an old crack in the bottom layer for all the samples. Besides, a neoprene rubber layer with an elasticity modulus of 11,000 kPa and a hardness of 65 was used as the bed soil in all tests [4, 24, 31–33].

## 2.3 Bending fatigue test method

The Haversian cyclic loading (load exactly on the crack) with the frequencies of 10, 6, and 2 Hz was performed on all samples at 0, 20, and 40 °C in duplicate using the Dynamic Creep Test software ver. 2.03. This kind of loading mode simulates high, medium, and low speed traffics [34]. The maximum value of the loading was equal to 6.9 kN (the compressive stress of 690 kPa). The loading was applied by the UTM25 apparatus (Fig. 4).

## 2.4 Image analysis

Two cameras located next to the sample continuously captured the pictures with 60 frames per seconds of the reflective cracks during the test and to better observe the cracks in the image analyzing, the side surfaces of the top layer was painted with white plastic construction paint (see Fig. 4). The test was terminated when the top layer of sample was cracked entirely, or in other words the reflective cracks passed the entire thickness. At the beginning of the tests, detecting the crack on the sample is very difficult, and the crack propagation is not visible to the eyes. In the crack initiation stage, the number of cracks is low, and mainly they are micro-crack type. Then, these cracks become wider and macro-cracks. As soon as starting the test, the cameras were taking pictures with a time interval of 1 s. Afterward, analyzing the captured pictures provides a good insight into the shape and process of reflective cracks, the time of initiation, and how the crack spreads in the overlay (see Fig. 5). Standard rulers are used



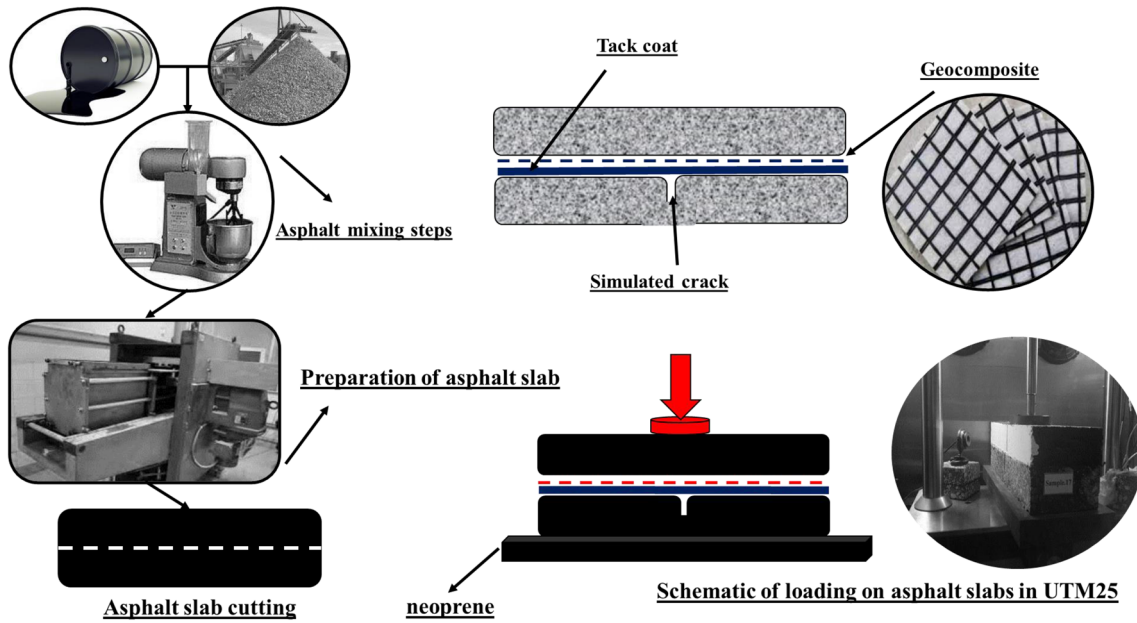


Fig. 3 Schematic view with details of the preparation steps of the double-layer asphalt sample with the geocomposite interlayer in the dynamic bending loading test

Fig. 4 Bending fatigue test configuration on the two-layer asphalt specimen

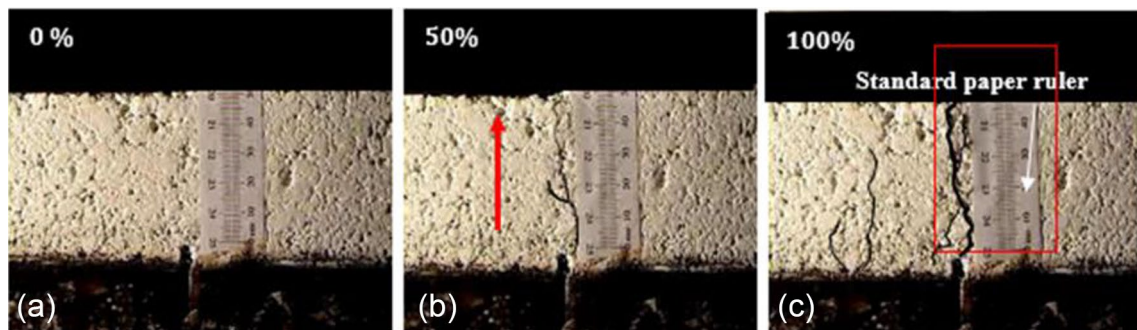
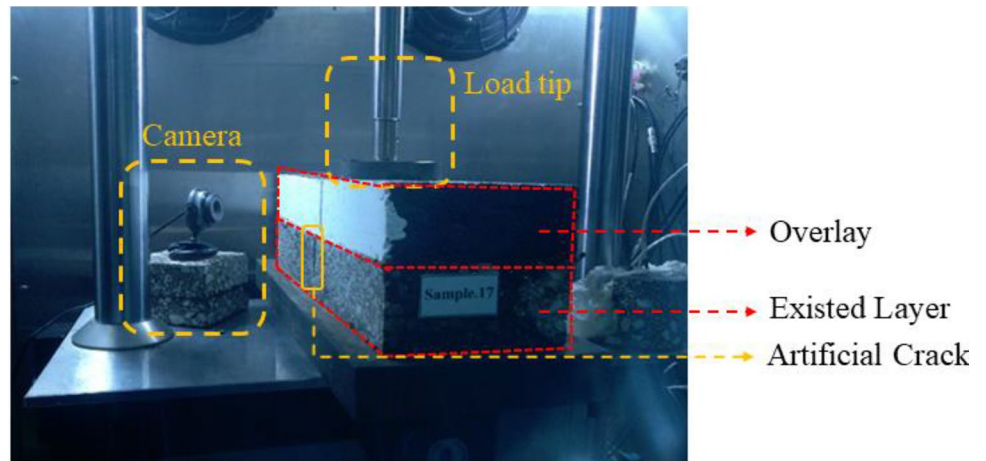


Fig. 5 Crack propagation appearance at three failure times: **a** at the time of load applies, **b** 50% of failure time, and **c** at failure time

to measure the cracking rate in the overlay. Therefore, it is possible to obtain the average crack penetration rate in the overlay by extracting the length of the crack penetration at the certain time intervals.

## 2.5 Design of experiment using statistical methods

In this research, Design-Expert software was used to analyze the data obtained from the results of the experiments. Generally, this software is used for designing the experiments, statistical analysis, and optimization. The independent variables considered in this research were the temperature, frequency and the type of geocomposite, and the dependent variable was the cracking rate. The software presents a model according to the information obtained from the analysis of variance (ANOVA) [35–38]. Moreover in this research, the results of the experiments were analyzed using the response surface method (RSM). The coefficient of determination ( $R^2$ ) and the lack of fit (LOF) are commonly presented to show the model's validity [39, 40]. The LOF indicates that how much the points are not well distributed around the model, and the model cannot be used to predict the dependent variable. Therefore, with the non-significance of the LOF test, it can be said that the model has been well fitted to the data. In addition,  $R^2$  is expressed as the ratio of the changes predicted by the model to the total changes, which is a measure of the

degree of fit. The closer  $R^2$  value to 1, the more powerful model which can describe the response changes as a function of independent variables [41, 42].

## 3 Results and discussion

After the sample preparation, they were subjected to fatigue loadings in different conditions along with capturing images. Then using image analyzing the following results were obtained.

### 3.1 Performance of asphalt slabs at 0°C

The results of image analysis show that the cracks in all reinforced and control samples at 0°C propagate at a very low rate and in the form of microcracks from the bottom to the top of the overlay. In the control samples, after loading, the cracks initiate exactly from the crack gap, move upward, and reach the overlay surface at a very low speed. The investigations also showed that in samples reinforced with geocomposite of type-I (see Fig. 6) and type-II (see Fig. 7), the cracks grow slower compared to cracks in the control ones. These cracks initiate at a small distance from the simulated crack location and then move upward in the form of microcracks

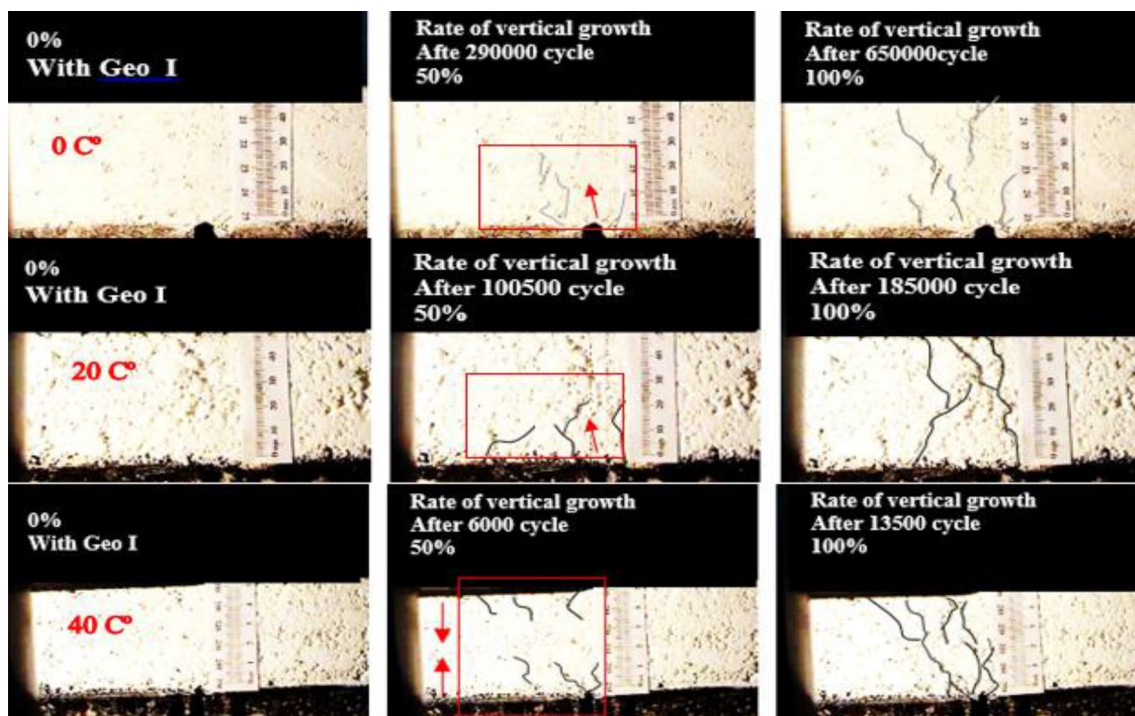


**Fig. 6** Cracking image in the asphalt slabs reinforced with type-I geocomposite under loading with a frequency of 10 Hz at 0, 20, and 40°C with a crack width of 12 mm



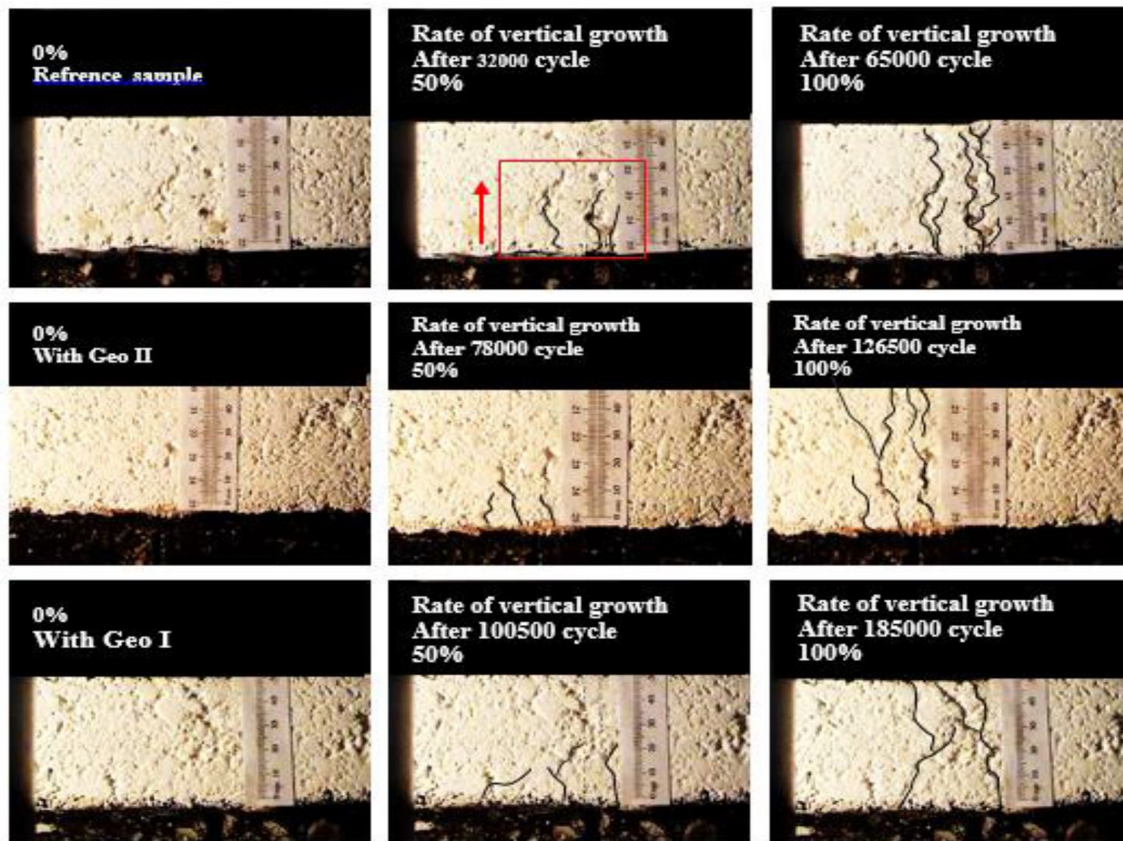


**Fig. 7** Cracking image in the control sample and the ones reinforced with type-I and II geocomposites under loading with a frequency of 10 Hz at 20°C with a crack width of 12 mm

and reach the overlay surface. Moreover, they usually propagate in several branches in the thickness of the overlay.

According to the calculations using the image analysis shown in Table 3, the vertical cracking rate ( $\text{mm}/\text{cycle} \times 10^{-4}$ ) at 0°C is very low in the control samples. By increasing the frequency from 2 to 6 and 10 Hz, the cracking rate increases by about 1.2 to 1.4 times, respectively. The growth of the cracks in reinforced overlays with type-I and II geocomposites is observed with a low rate, too. But, with the increase in the loading intensity from 2 to 6 and 10 Hz, the cracking rate increases by 1.25 to 1.45 times in samples reinforced with type-I geocomposite and 1.35 to 1.55 times in samples reinforced with type-II geocomposite, respectively. The decrease in cracking rate at 0°C in samples reinforced with type-II geocomposite compared to control samples was observed by almost 30% in all frequencies. But, more reduction (55 to 60%) occurred in the cracking rate in samples reinforced with type-I geocomposite in different frequencies. This result represents the appropriate performance of the type-I geocomposite in reinforcing asphalt overlays and delay in the reflective cracking at 0°C.

### 3.2 Performance of asphalt slabs at 20°C

The results of image processing revealed that the cracks move from the bottom of overlay to its top in all samples like what was observed in 0°C. At first, the cracks are micro type but shortly turn into one or two main macrocracks. In the control samples, after loading, the cracks initiate exactly from the crack gap in the bottom layer, move upward, and reach the overlay surface at a medium speed. The cracks in slabs reinforced with type-II geocomposite initially grow at a low speed as microcracks, slightly away from the simulated crack. Then, after passing the half of the overlay thickness, one or two main branches grow and appear as macrocracks. It should be mentioned that after 50% of crack growth, the vertical growth rate also increases. The cracks in slabs reinforced with type-I geocomposite move at a very low speed. Similar to the control samples reinforced with type-II geocomposite, the initial cracks are micro type. But, unlike them, in this case the cracks grow as a group of cracks and the width of several branches during loading increases. In addition, the crack opening width in samples reinforced with type-I geocomposite is less than the other samples (Fig. 7). According to

**Table 3** Fatigue bending test result under different load frequencies at 0, 20, and 40°C

Test No	Sample type	Frequency (Hz)	temperature (°C)	Maximum vertical displacement (mm)	Vertical growth rate; (mm/cycle) × 10 <sup>-4</sup>
Test 1	Control	2	0	1.78	1.3
Test 2	Control	6	0	2.17	1.6
Test 3	Control	10	0	2.34	1.8
Test 4	Reinforced with composite type-I	2	0	2.53	0.9
Test 5	Reinforced with composite type-I	6	0	2.8	1.1
Test 6	Reinforced with composite type-I	10	0	3.01	1.3
Test 7	Reinforced with composite type-II	2	0	2.43	0.52
Test 8	Reinforced with composite type-II	6	0	2.63	0.7
Test 9	Reinforced with composite type-II	10	0	2.88	0.8
Test 10	Control	2	20	2.24	6.5
Test 11	Control	6	20	2.86	7.6
Test 12	Control	10	20	3.12	8.7
Test 16	Reinforced with composite type-I	2	20	3.2	1.6
Test 17	Reinforced with composite type-I	6	20	3.33	2.7
Test 18	Reinforced with composite type-I	10	20	3.76	3
Test 13	Reinforced with composite type-II	2	20	3.2	3.5
Test 14	Reinforced with composite type-II	6	20	3.7	4
Test 15	Reinforced with composite type-II	10	20	3.99	6
Test 19	Control	2	40	3.26	33.3
Test 20	Control	6	40	3.5	38.7
Test 21	Control	10	40	3.88	47.5
Test 25	Reinforced with composite type-I	2	40	4.1	24.6
Test 26	Reinforced with composite type-I	6	40	4.65	29.75
Test 27	Reinforced with composite type-I	10	40	4.89	37.5
Test 22	Reinforced with composite type-II	2	40	3.92	28.6
Test 23	Reinforced with composite type-II	6	40	4.14	31.9
Test 24	Reinforced with composite type-II	10	40	4.52	40.1

the image analysis results (Table 3), the vertical cracking rate at this temperature is much lower for reinforced overlays compared to control ones.

The vertical cracking rate in overlays reinforced with type-II geocomposite compared to control samples is 31 to 47%. Meanwhile, in samples reinforced with type-I geocomposite, this rate has decreased by 64 to 75% compared to control samples in different frequencies. This outcome indicates the better performance of type-I geocomposite similar to 0°C.

### 3.3 Performance of asphalt slabs at 40°C

Unlike what was seen in 0 and 20°C, the cracks move from the top and bottom of the overlay to its middle part at 40°C in control asphalt slabs. The cracks are initially formed as microcracks, and after reaching the middle of the overlay, they widen quickly and turn into macrocracks. This change in the cracking process and its initiation direction

are related to the temperature rise, the weak adhesion of stone materials to bitumen, or the increase in viscosity and fluidity of the bitumen in the asphalt mixture. It is of note that the cracking rate to reach the overlay surface is very fast at this temperature. Cracks in slabs reinforced with type-II geocomposite at 40°C first move as microcracks from the top and bottom of the overlay to its middle zone. Afterward, they widen rapidly and covers the entire overlay. The results showed that the cracks grow at a slower rate in the samples reinforced with type-II geocomposite than the control reference samples. The cracking process in the slabs reinforced with type-I geocomposite is similar to type-II geocomposite process, except that the cracks in samples reinforced with type-I geocomposite grow at a slower rate than the samples reinforced with type-II geocomposite. According to Table 3, the vertical cracking rate is very high in reinforced and non-reinforced overlays at 40°C. Also, by increasing the loading rate from 2 to 6 and 10 Hz, the cracking rate increases from 1.16 to 1.43 times,



**Table 4** Coding the research variables in design-expert software

Temperature = A		
LEVELS	- 1	1
Temperature (°C)	0	40
Frequency = B		
LEVELS	- 1	1
Frequency (Hz)	2	10
Type of geosynthetic = C		
LEVELS	C[1]	C[2]
GOE I	- 1	- 1
GOE II	0	1
WITHOUT GEO	1	0

respectively. The assessments showed that the vertical rate of cracking in overlays reinforced with type-II geocomposite has decreased by 14 to 18% compared to the control samples. On the other hand, the vertical cracking rate in overlays reinforced with type-I geocomposite has decreased by 26–27% compared to the control samples. Also, with increasing the loading intensity from 2 to 6 and 10 Hz, the cracking rate increases approximately from 1.21 to 1.52 times. Comparing the cracking rate reduction for all samples, it is revealed that the type-I geocomposite shows better performance than type-II one at 40°C.

### 3.4 Statistical analysis and presentation of vertical cracking rate regression models in anti-crack multi-layered asphalt pavements

The statistical analysis was performed based on RSM and the historical data in the Design-Expert 12 software. The vertical cracking rate was analysed based on the following independent variables: temperature (T=A), frequency (F=B), and type of interlayer (G=C), as shown in Table 4.

ANOVA results based on the fitting criteria including the degrees of freedom in the source (DF), the sum of squares due to the source (SS), the mean sum of squares due to the source (MS), P-values, and R<sup>2</sup> are presented in Table 5. As can be seen, the P-value was acceptable for all independent variables (P < 0.05). Also, P-values for variables AB and AC were smaller than 0.05. In other words, all the variables are significant at the 95% confidence level, indicating that all the research variables are influential in the model. One of the advantages of statistical analysis compared to other analytical methods is the simultaneous examination of the interaction or mutual effect of each variable on the response, which was done in this research. The F-value (F-statistic) of the presented model is equal to 170.99, indicating the model's good acceptability for describing the response. R<sup>2</sup> and R<sup>2</sup>-adj as the two most important prediction assessment criteria were obtained 0.9936 and 0.9907, respectively. These high values indicate the satisfactory accuracy of that model. Equation (1) presents the extracted model in coded form.

#### Rate of vertical growth

$$= 4.84 + 16.77 \times A + 2.55 \times B + 2.79 \times C[1] - 1.47 \times C[2] + 3.12 \times A \times B + 2.36 \times A \times C[1] - 2.02 \times A \times C[2] + 13.04 \times A^2 \tag{1}$$


Figure 8 depicts the graph of the predicted values against the actual ones. The results show the acceptable accuracy of the fitted model predicting the cracking rate as the response against the actual values obtained from the experiment. Also, Fig. 9 shows the effect of independent variables and their interaction on the cracking rate. According to the presented cracking rate model and examining the coefficients of their effect, the temperature will have the most significant impact on the response. Also, among the investigated variables in the cracking rate model, temperature and frequency increase

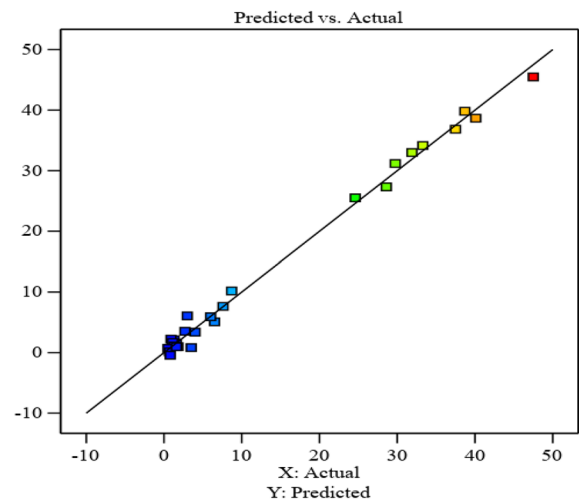
**Table 5** ANOVA results of the model to predict the reflective cracking rate and the importance of each parameter

Source	Sum of squares	df	Mean square	F-value	P-value	Significant?
model	6.48E+03	8	8.10E+02	348.92	<0.0001	Yes
A-T	5064.54	1	5064.54	2180.67	<0.0001	Yes
B-F	116.94	1	116.94	50.35	<0.0001	Yes
C-G	105.45	2	52.73	22.7	<0.0001	Yes
AB	116.69	1	116.69	50.24	<0.0001	Yes
AC	58.49	2	29.24	12.59	0.0004	Yes
A <sup>2</sup>	1020.68	1	1020.68	439.48	<0.0001	Yes
Residual	41.8	18	2.32			
Cor total	6524.6	26				
R <sup>2</sup>	0.9936					
Adjusted R <sup>2</sup>	0.9907					

**Fig. 8** Predicted values of cracking rate by the statistical model against the actual values

### Rate of vertical growth

Color points by value of Rate of vertical growth:  
0.52  47.5



the response, while geosynthetic type-I decreases it (Fig. 9a–c). Figure 9d shows the interaction of temperature and frequency on the response variable. As can be seen with increasing the temperature, the samples were loaded with higher frequency experience the higher cracking rates. According to Fig. 9e, the samples reinforced with geocomposites show a lower cracking rate at a constant frequency with increasing temperature. As the temperature rises, this interlayer decreases the cracking rate more considerably.

In this research based on the sensitivity analysis, the influence of the independent inputs on the dependent outputs (responses) for the reinforced and unreinforced asphalt overlays has been investigated through the obtained statistical model. In other words, with this method the sensitivity of the output variable can be determined over an each input variable. According to the output of the sensitivity analysis shown in Fig. 10, it can be seen that in comparison to other parameters the temperature has the greatest effect on the control of reflective cracks and changes in the crack growth rate in reinforced and unreinforced asphalt samples. After that, the type of geocomposite and then the loading intensity will have the greatest effect on the increasing the crack growth rate.

## 4 Conclusion

This paper studies the effects of temperature changes, the intensity of loading frequency, and the type of geocomposite on the vertical cracking rate and vertical deformation, followed by the statistical analysis of the laboratory data. According to the obtained data and analysis, the major results of this study are outlined as follows:

- At all loading intensities and temperatures, the samples reinforced with type-I geocomposite have shown the better performance in reduction of cracking rate than those reinforced samples with type-II geocomposite and control ones.
- In the crack initiation stage, the number of cracks is low, and the defects are of microcrack type. Next, these cracks become wider and turn into macrocracks. Also, the cracking form in control samples is usually single-branched mode with a large crack width (due to high stress concentration on the crack). But in reinforced samples, the cracks propagate in the form of microcracks with several branches in the areas far from the crack and spread slowly on the overlay surface. This outcome is attributed to the stress and strain reduction on the overlay surface which is achieved by reinforcing the pavement with the high tensile strength geocomposite.
- Based on the image processing results, the trend and shape of crack growth in reinforced and non-reinforced samples change extremely at different temperatures and frequencies. Usually, at low temperatures and frequencies (0 and 20 °C), the cracks grow from the bottom to the top of the overlay and have a smaller width. While, with the increase in temperature from 20 to 40 °C, in addition to increasing the crack growth rate and changing the vertical deformation under the load, the direction of the cracks changes by the top to the bottom. The formation of top-down cracks depends on the increase in temperature and being influenceable of asphalt mixtures in these high temperature and frequency ranges.
- The change in the crack propagation process and its starting direction is caused by the increase in temperature and the weak adhesion of aggregate and asphalt

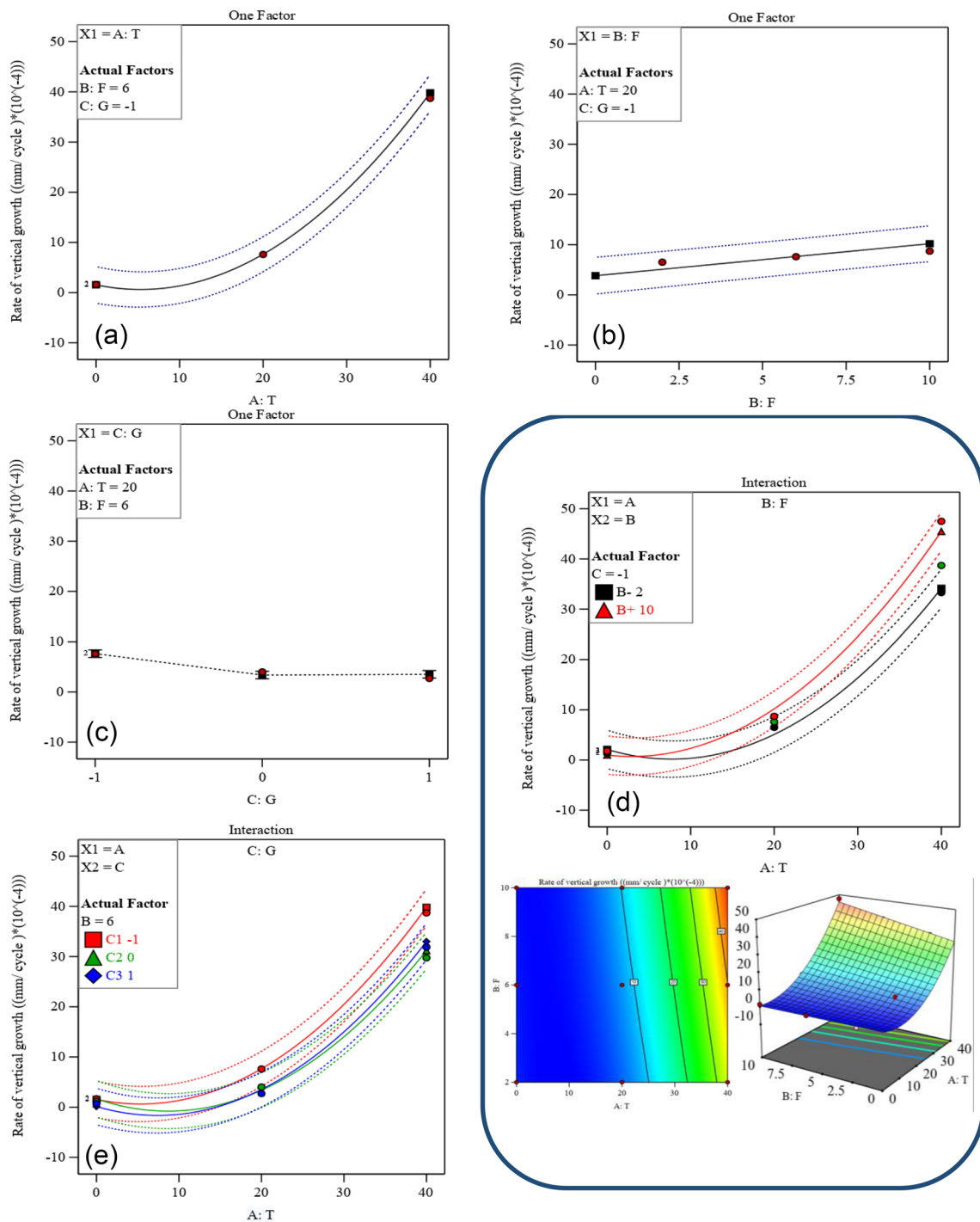


**Fig. 9** Effect of each variable independently and reciprocally on the cracking propagation rate, **a** crack growth rate against the temperature for 6 Hz frequency and type-I geocomposite, **b** crack growth rate against the frequency for 20 °C temperature and type-I geocomposite, **c** crack growth rate against the geocomposite types

for 20 °C temperature and 6 Hz frequency, **d** interaction of the temperature and frequency against the changes in crack growth rate in type-I geocomposite, **e** interaction of the temperature and geocomposite type against the crack growth rate changes at 6 Hz frequency.

and the decrease in bitumen viscosity. In other words, the destruction and cracks in asphalt pavements at high temperatures, in addition to the reflective bot-

tom cracks, are also caused by top-down destruction and cracks.

- It should be noted that the increase of the environment temperature will have a remarkable negative effect on



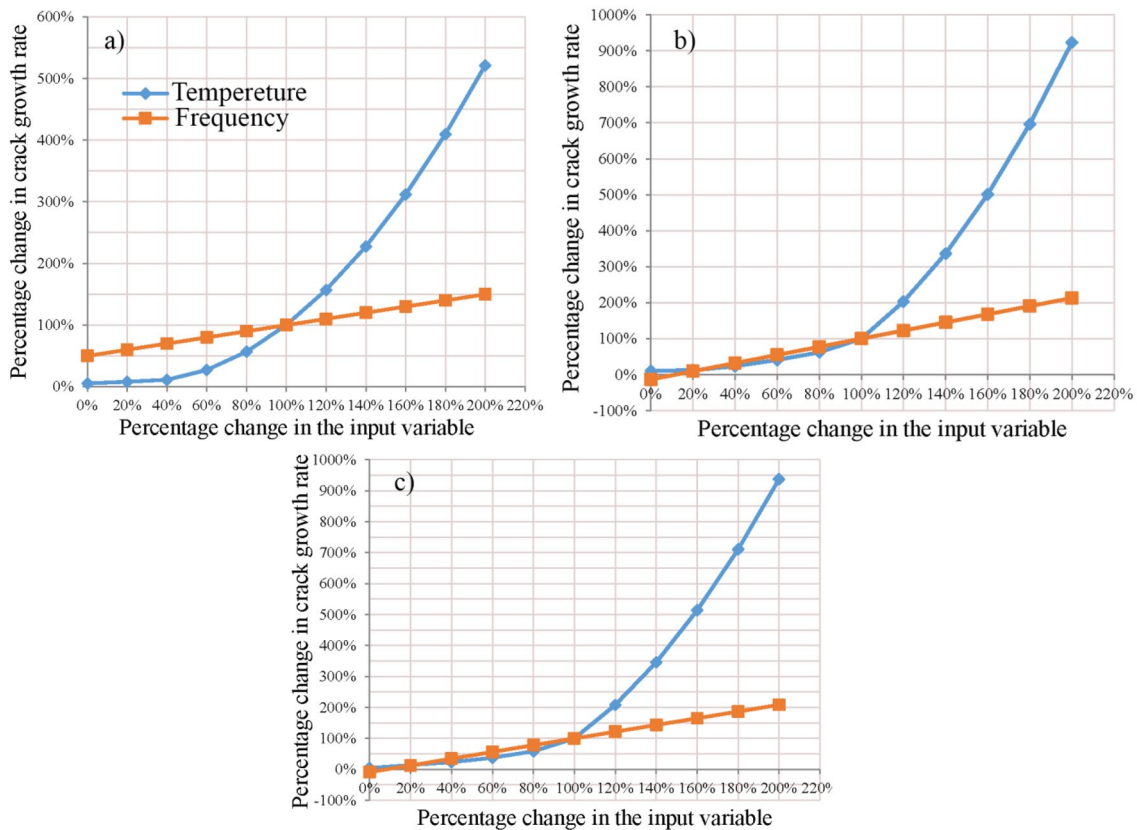


**Fig. 10** Sensitivity analysis based on the output change percentage relative to the input variables of temperature and loading frequency on asphalt samples: **a** reinforced with type-I geocomposite, **b** reinforced with type-II geocomposite, **c** control

the viscosity of the single-coat layer and the adhesion between the overlay and the geocomposite, and reduces the performance of the reinforcing intermediate layer.

- The temperature has the greatest effect on the control of reflective cracks in both reinforced and control samples. After that, the type of geosynthetic and the loading rate are the effective parameters, respectively.
- The crack growth rate in all studied temperatures is the highest for the control samples. Also, increasing the loading frequency and temperature, in reinforced and control samples, increases that rate. Moreover, the high strength geocomposite (100 kN.m) has shown the greatest effect on improving the performance of asphalt pavement in reducing the crack penetration rate in all temperatures.
- By comparing the graphs of the crack growth rate at all temperatures and frequencies, it is revealed that the lowest crack growth rate corresponds to the samples tested at 0 and 20 °C. A part of this reduction is related to the performance of geocomposite layers at low tem-

peratures and the other part is related to the resistance increase of the asphalt beams at low temperatures.

- The  $R^2$  and  $R^2$ -adj values obtained in the model to estimate the cracking rate based on the temperature, frequency, and geocomposite type are 0.9936 and 0.9907, respectively, which indicating the high accuracy of model.
- According to the result of prediction model and analysis of variance, the P-values for all variables are significant in 95% confidence level. In other words, this indicates that the considered variables are effective in the presented quadratic models.
- The statistical analysis showed that the interaction of temperature and frequency also affects the cracking rate. Furthermore, as the temperature rises, the samples loaded with higher frequency show the higher cracking rate.

**Author contributions** saeid asadi conceived of the presented idea, developed the theory and performed the computations ,conceived

and planned the experiments and carried out the experiments. gholamali shafabakhsh developed the theoretical formalism, performed the analytic calculations, performed the numerical simulations and wrote the manuscript.

**Data availability** All data supporting the findings of this study are presented in this article. Any additional data can be obtained from the corresponding author upon reasonable request.

## Declarations

**Conflict of interest** The authors declare that they have no known competing financial interests or personal relationships that could have appeared to influence the work reported in this paper.

**Open Access** This article is licensed under a Creative Commons Attribution 4.0 International License, which permits use, sharing, adaptation, distribution and reproduction in any medium or format, as long as you give appropriate credit to the original author(s) and the source, provide a link to the Creative Commons licence, and indicate if changes were made. The images or other third party material in this article are included in the article's Creative Commons licence, unless indicated otherwise in a credit line to the material. If material is not included in the article's Creative Commons licence and your intended use is not permitted by statutory regulation or exceeds the permitted use, you will need to obtain permission directly from the copyright holder. To view a copy of this licence, visit <http://creativecommons.org/licenses/by/4.0/>.

## References

1. De Bondt A (1999) Introduction. Anti-reflective cracking design of reinforced (reforced) asphaltic overlays, Thesis, Delft University of Technology. Holanda. <https://www.elibrary.ru/item.asp?id=6887356>
2. Idris II, Sadek H, Hassan M (2020) State-of-the-art review of the evaluation of asphalt mixtures' resistance to reflective cracking in laboratory. *J Mater Civil Eng* 32(9):20004. [https://doi.org/10.1061/\(ASCE\)MT.1943-5533.0003254](https://doi.org/10.1061/(ASCE)MT.1943-5533.0003254)
3. Germann FP, Lytton RL (1979) Methodology for predicting the reflection cracking life of asphalt concrete overlays. <https://library.ctr.utexas.edu/digitized/texasarchive/207-5.pdf>
4. Khodaii A, Fallah S, Nejad FM (2009) Effects of geosynthetics on reduction of reflection cracking in asphalt overlays. *Geotext Geomembr* 27(1):1–8. <https://doi.org/10.1016/j.geotextmem.2008.05.007>
5. Dave EV, Buttlar WG (2010) Thermal reflective cracking of asphalt concrete overlays. *Int J Pavement Eng* 11(6):477–488. <https://doi.org/10.1080/10298430903578911>
6. De Bondt AH (2000) Anti-reflective cracking design of (reinforced) asphaltic overlays. <https://www.elibrary.ru/item.asp?id=6887356>
7. Bozkurt D (2002) Three-dimensional finite element analysis to evaluate reflective cracking potential in asphalt concrete overlays: University of Illinois at Urbana-Champaign. OCLC Number/Unique Identifier: 51635691
8. Button J, Lytton R, Cleveland G Product 0-1777-p2 project number 0-1777 research project title: field synthesis of geotextiles in flexible and rigid pavement overlay strategies including cost considerations. <https://static.tti.tamu.edu/tti.tamu.edu/documents/0-1777-P2.pdf>
9. Francken L, Beuving E, Molenaar AAA (2004) Reflective cracking in pavements: design and performance of overlay systems. CRC Press, Boca Raton. <https://doi.org/10.1201/9781482271799>
10. Perez SA, Balay JM, Tamagny P, Petit Ch (2007) Accelerated pavement testing and modeling of reflective cracking in pavements. *Eng Fail Anal* 14(8):1526–1537. <https://doi.org/10.1016/j.engfailanal.2006.12.010>
11. Loria-Salazar LG (2008) Reflective cracking of flexible pavements: literature review, analysis models, and testing methods. University of Nevada, Reno
12. Kim YR (2009) Modeling of asphalt concrete: McGraw-Hill Education. ISBN: 9780071464628
13. Button JW, Lytton RL (2007) Guidelines for using geosynthetics with hot-mix asphalt overlays to reduce reflective cracking. *Transp Res Rec* 2004(1):111–119
14. Zhang Ke, Zhang Z, Luo Y (2018) Material composition design and anticracking performance evaluation of asphalt rubber stress-absorbing membrane interlayer (AR-SAMI). *Adv Mater Sci Eng*. <https://doi.org/10.1155/2018/8560604>
15. Hosseini HRA, Darban AK, Fakhri K (2009) The effect of geosynthetic reinforcement on the damage propagation rate of asphalt pavements. <https://www.sid.ir/en/journal/ViewPaper.aspx?id=141151>
16. Maurer DA, Malasheskie GJ (1989) Field performance of fabrics and fibers to retard reflective cracking. *Geotext Geomembr* 8(3):239. [https://doi.org/10.1016/0266-1144\(89\)90005-8](https://doi.org/10.1016/0266-1144(89)90005-8)
17. Elseifi MA, Al-Qadi IL (2005) Modeling of strain energy absorbers for rehabilitated cracked flexible pavements. *J Transp Eng* 131(9):653–661. [https://doi.org/10.1061/\(ASCE\)0733-947X\(2005\)131:9\(653\)](https://doi.org/10.1061/(ASCE)0733-947X(2005)131:9(653))
18. Shafabakhsh G, Akbari M, Bahrami H (2020) Evaluating the fatigue resistance of the innovative modified-reinforced composite asphalt mixture. *Adv Civil Eng*. <https://doi.org/10.1155/2020/8845647>
19. Ingrassia LP, Virgili A, Canestrari F (2020) Effect of geocomposite reinforcement on the performance of thin asphalt pavements: accelerated pavement testing and laboratory analysis. *Case Stud Constr Mater* 12:e00342. <https://doi.org/10.1016/j.cscm.2020.e00342>
20. Saraf CL, Majidzadeh K (1974) Dynamic response and fatigue characteristics of asphaltic mixtures: ASTM International. <https://www.astm.org/stp32178s.html>
21. Saraf CL, Majidzadeh K, Tribbett WO (1996) Effect of reinforcement on fatigue life of asphalt beams. *Transp Res Rec* 1534(1):66–71
22. Çelik M, Seferoğlu MT, Akpınar MV (2021) Performance of AC overlays using geogrids on PCC contraction joints. *Geotext Geomembr* 49(4):1058–1065. <https://doi.org/10.1016/j.geotextmem.2021.02.004>
23. Dizaj AB, Ziari H, Nejhad MA (2014) Effects of carbon fibre geogrid reinforcement on propagation of cracking in pavement and augmentation of flexible pavement life. *Adv Mater Res*. <https://doi.org/10.4028/www.scientific.net/AMR.891-892.1533>
24. Fallah S, Khodaii A (2015) Evaluation of parameters affecting reflection cracking in geogrid-reinforced overlay. *J Central S Univ* 22(3):1016–1025. <https://doi.org/10.1007/s11771-015-2612-9>
25. Tam AB, Park D-W, Le THM, Kim J-S (2020) Evaluation on fatigue cracking resistance of fiber grid reinforced asphalt concrete with reflection cracking rate computation. *Constr Build Mater* 239:117873. <https://doi.org/10.1016/j.conbuildmat.2019.117873>
26. Solatiyan E, Bueche N, Carter A (2021) Laboratory evaluation of interfacial mechanical properties in geogrid-reinforced

- bituminous layers. *Geotext Geomembr* 49(4):895–909. <https://doi.org/10.1016/j.geotextmem.2020.12.014>
27. Sina MM, Mohamed RK, Abdelaziz M, Ali K (2011) An overview on the use of geosynthetics in pavement structures. *Sci Res Essays* 6(11):2234–22418. <https://doi.org/10.5897/SRE10.960>
  28. Berg RR (2000) Geosynthetic reinforcement of the aggregate base/subbase courses of pavement structures. <https://rosap.nrl.bts.gov/view/dot/29464>
  29. Ling HI, Liu Z (2001) Performance of geosynthetic-reinforced asphalt pavements. *J Geotech Geoenviron Eng* 127(2):177–184. [https://doi.org/10.1061/\(ASCE\)1090-0241\(2001\)127:2\(177\)](https://doi.org/10.1061/(ASCE)1090-0241(2001)127:2(177))
  30. Gonzalez-Torre I, Calzada-Perez MA, Vega-Zamanillo A, Castro-Fres D (2015) Experimental study of the behaviour of different geosynthetics as anti-reflective cracking systems using a combined-load fatigue test. *Geotext Geomembr* 43(4):345–350. <https://doi.org/10.1016/j.geotextmem.2015.04.001>
  31. Nejad M, Fereidoon AN, Toolabi S, Fallah S (2015) Effect of using geosynthetics on reflective crack prevention. *Int J Pavement Eng* 16(6):477–487. <https://doi.org/10.1080/10298436.2014.943128>
  32. Nejad FM, Asadi S, Fallah S, Vadood M (2016) Statistical-experimental study of geosynthetics performance on reflection cracking phenomenon. *Geotext Geomembr* 44(2):178–187. <https://doi.org/10.1016/j.geotextmem.2015.09.002>
  33. Noory A, Nejad FM, Khodaii A (2019) Evaluation of geocomposite-reinforced bituminous pavements with Amirkabir University Shear Field Test. *Road Mater Pavement Des* 20(2):259–279. <https://doi.org/10.1080/14680629.2017.1380690>
  34. Hu S, Hu X, Zhou F (2008) Using semi-analytical finite element method to evaluate stress intensity factors in pavement structure. *Pavement Crack*. <https://doi.org/10.1201/9780203882191.ch62>
  35. Khodaii A, Haghshenas HF, Kazemi Tehrani H (2012) Effect of grading and lime content on HMA stripping using statistical methodology. *Constr Build Mater* 34:131–135. <https://doi.org/10.1016/j.conbuildmat.2012.02.025>
  36. Khuri AI, Mukhopadhyay S (2010) Response surface methodology. *Wiley Interdiscip Rev* 2(2):128–149. <https://doi.org/10.1002/wics.73>
  37. Myers RH, Khuri AI, Carter WH (1989) Response surface methodology: 1966–1988. *Technometrics* 31(2):137–157. <https://doi.org/10.1080/00401706.1989.10488509>
  38. Usman A, Sutanto MH, Napiah M, Zoorob SE, Abdulrahman S, Saeed SM (2021) Irradiated polyethylene terephthalate fiber and binder contents optimization for fiber-reinforced asphalt mix using response surface methodology. *Ain Shams Eng J* 12(1):271–282. <https://doi.org/10.1016/j.asej.2020.06.011>
  39. Bala N, Napiah M, Kamaruddin I (2020) Nanosilica composite asphalt mixtures performance-based design and optimisation using response surface methodology. *Int J Pavement Eng* 21(1):29–40. <https://doi.org/10.1080/10298436.2018.1435881>
  40. Usman A, Sutanto MH, Napiah MB, Yaro NSA (2021) Response surface methodology optimization in asphalt mixtures: a review. *Response Surf Methodol Eng Sci*. <https://doi.org/10.5772/intechopen.95994>
  41. Zhang P, Cheng YC, Tao JL, Jiao YB (2016) Molding process design for asphalt mixture based on response surface methodology. *J Mater Civ Eng* 28(11):04016120. [https://doi.org/10.1061/\(ASCE\)MT.1943-5533.0001640](https://doi.org/10.1061/(ASCE)MT.1943-5533.0001640)
  42. Bala N, Kamaruddin I, Napiah M, Sutanto MH (2019) Polymer nanocomposite-modified asphalt: characterisation and optimisation using response surface methodology. *Arab J Sci Eng* 44(5):4233–4243. <https://doi.org/10.1007/S13369-018-3377-X>

**Publisher's Note** Springer Nature remains neutral with regard to jurisdictional claims in published maps and institutional affiliations.